SUPPORTING INFORMATION

Nanocrystalline $TiO_2/Ti_3C_2T_x$ MXene composites with tunable work function prepared using atmospheric pressure oxygen plasma

Július Vida[1], Pavol Gemeiner[2], Michaela Pavličková[2], Martina Mazalová[1], Pavel Souček[1], Dušan Plašienka[1] and Tomáš Homola[1]

[1] Department of Physical Electronics, Faculty of Science, Masaryk University, Kotlářská 267/2, 611 37 Brno, Czech Republic

[2] Department Graphical Arts Technology and Applied Photochemistry, Faculty of Chemical and Food Technology, Slovak University of Technology in Bratislava, Radlinského 9, 812 37 Bratislava, Slovakia

Surface chemistry

X-ray photoelectron spectroscopy (XPS) was used to analyse surface chemistry and bonding states on the surface of MXenes. Atomic concentrations of elements on the surface detected by XPS are shown in **Table S1**. Titanium, carbon, oxygen, and fluorine were detected. Titanium and carbon form the MXene sheets and oxygen, and fluorine are present as functionalities bonded to the surface Ti atoms.

We also analysed the narrow core-level regions in XPS of Ti 2p, C 1s, O 1s and F 1s. The fitting of measured spectra was done according to the algorithm proposed by *Natu et al.* [1]. All components, peak positions, and components' shares of the intensity of the spectrum are summarized in **Table S2** and the evolution of components' shares as a function of plasma treatment time is shown in **Figure S1**.

The deconvolutions of Ti 2p core-level spectra are shown in **Figure S2**. The Ti 2p region is known to exhibit the effect of spin-orbit splitting manifesting in doublets of all peaks labelled as Ti 2p 3/2 and Ti 2p 1/2. The Ti 2p regions of MXenes analysed in this work displayed a broad asymmetrical peak at around 456 eV and a symmetrical peak at around 459.5 eV. The lower binding energy peak was fitted with four components at 455.2 eV, 456.1 eV, 457.1 eV and 458.1 eV corresponding to different Ti environments in the MXene, distinguished by the atoms of oxygen and fluorine bonded to Ti. Specifically, the peak at 455.2 eV corresponds to Ti bonded to three O atoms labelled C—Ti—O/O/O, the peak at 456.1 eV corresponds to Ti bonded to two O atoms and one F atom labelled C—Ti—O/O/F, the peak at 457.1 eV represents Ti bonded to one O and two F atoms marked as C—Ti—O/F/F and finally the peak at 458.1 eV stems from Ti bonded to three F atoms labelled C—Ti—F/F/F. The peak at 495.5 eV was assigned to oxyfluoride species $TiO_{2-x}F_{2x}$ that form as the MXene oxidizes either by contact with

Table S1. Atomic concentrations on MXene samples before and after oxygen plasma treatment, detected by XPS

Treatment time [s]	Titanium [%]	Carbon [%]	Oxygen [%]	Fluorine [%]
0	22.6 ± 0.2	32.9 ± 0.2	33.1 ± 0.6	11.5 ± 0.2
1	19.1 ± 0.2	28.8 ± 0.4	41.7 ± 0.3	10.5 ± 0.3
8	16.0 ± 0.4	27.9 ± 0.5	43 ± 1	13 ± 2
32	21.2 ± 0.1	24.3 ± 0.3	44.6 ± 0.1	9.9 ± 0.4
64	18.1 ± 0.1	24.5 ± 0.1	46.5 ± 0.2	10.98 ± 0.06
128	20.6 ± 0.3	23.3 ± 0.3	44.4 ± 0.3	11.7 ± 0.3

oxygen-containing atmosphere or by further plasma treatment. The four peaks arising from the MXene were modelled using asymmetrical line shapes due to the conductive nature of MXene. The $TiO_{2-x}F_{2x}$ peak was represented by symmetrical gaussian-lorentzian line shape. At higher binding energies we observed the Ti 2p 1/2 counterparts for the peaks. The peak separation between the Ti 2p 3/2 and 1/2 was maintained at 6.1 eV for the MXene peaks and 5.6 eV for the oxyfluoride peak. In **Figure S2a – Figure S2f** the deconvolutions for the untreated MXene and plasma-treated MXene for 1 – 128 s are shown. We observed fast decrease of the intensity of the MXene peaks and the oxyfluoride peak dominated the spectrum for longer treatment times. The evolution of the components' shares as a function of the plasma treatment time is shown in **Figure S1a**.

The deconvolutions of the C 1s core-level XPS spectra of untreated and plasma-treated MXene coatings are shown in **Figure S3**. Four components were used for the fitting at 282.0 eV, 285.4 eV, 287.0 eV and 289.1 eV corresponding to carbon bonded to titanium in the MXene, carbon in C—C/C—H, carbon in C—OH and carbon in O—C=O environments of the surface contamination, respectively. The Ti—C component representing MXene was modelled with an asymmetrical line shape, the peaks from carbon surface contamination were fitted by symmetrical components. After the plasma treatment we observed an exponential decrease in the intensity of the

Table S2. Components' shares obtained from fitting core-level spectra from XPS

Treatment time		**0 s**	**1 s**	**8 s**	**32 s**	**64 s**	**128 s**
Ti 2p [%]	C—Ti—O/O/O 3/2: 455.2(1) eV 1/2: 461.2(1) eV	27.4 ± 0.6	21.1 ± 0.2	13.0 ± 0.1	7.5 ± 0.6	7.4 ± 0.3	7.1 ± 0.1
	C—Ti—O/O/F 3/2: 456.1(1) eV 1/2: 462.2(2) eV	14.7 ± 0.4	9.3 ± 0.5	6.1 ± 0.1	1.9 ± 0.8	3.5 ± 0.6	1.6 ± 0.2
	C—Ti—O/F/F 3/2: 457.1(1) eV 1/2: 463.1(1) eV	15.1 ± 0.8	6.3 ± 0.1	6.4 ± 0.9	5.1 ± 0.2	4.4 ± 0.4	4.8 ± 0.1
	C—Ti—F/F/F 3/2: 458.1(1) eV 1/2: 464.2(1) eV	5.6 ± 0.1	2.5 ± 0.6	2.1 ± 0.4	0 ± 0	0.1 ± 0.1	0.6 ± 0.6
	TiO_2/ $TiO_{2-x}F_x$ 3/2: 459.5(2) eV 1/2: 465.1(2) eV	37 ± 2	60.1 ± 0.9	72 ± 1	85.6 ± 0.1	84.6 ± 0.5	86 ± 1
C 1s [%]	Ti—C 282.0(1) eV	30.1 ± 0.5	17 ± 1	12.8 ± 0.3	7.5 ± 0.3	10 ± 1	6.2 ± 0.1
	C—C/C—H 285.4(1) eV	55.0 ± 0.5	55.2 ± 0.3	64 ± 3	69.4 ± 0.2	71 ± 1	70.8 ± 0.1
	C—OH/C—O—C 287.0(1) eV	9.0 ± 0.3	13.7 ± 0.7	12 ± 2	14.5 ± 0.3	10.9 ± 0.2	14 ± 1
	O—C=O 289.1(2) eV	5.9 ± 0.3	14 ± 1	12 ± 1	8.6 ± 0.4	8.0 ± 0.1	9 ± 1
O 1s [%]	C—Ti—O 529.9(1) eV	7.6 ± 0.3	0.4 ± 0.4	0 ± 0	0 ± 0	0.7 ± 0.1	0.2 ± 0.2
	$TiO_{2-x}F_{2x}$ 530.7(1) eV	57.6 ± 0.8	59 ± 1	70 ± 2	75.1 ± 0.8	72.1 ± 0.1	73.6 ± 0.3
	C—Ti—OH C—Ti—O/F 531.9(3)	19.7 ± 0.1	24 ± 3	26 ± 2	21.8 ± 0.6	23.0 ± 0.6	21.6 ± 0.3
	H_2O/organic 533.7(1)	15 ± 1	16 ± 2	3.3 ± 0.6	3.1 ± 0.3	4.1 ± 0.4	4.7 ± 0.9
F 1s [%]	C—Ti—F 685.0(1) eV	100	100	100	100	100	100

Ti—C peak meaning a diminishing of the MXene structure of the film. The evolution of the components' shares is shown in **Figure S1b**.

The deconvolutions of the O 1s core-level XPS spectra of untreated and plasma-treated MXene coatings are shown in **Figure S4**. The spectra were fitted with four components at 529.9 eV, 530.7 eV, 531.9 eV and 533.7 eV. The most intensive peak at 530.7 eV comes from the oxide and oxyfluoride species $TiO_{2-x}F_{2x}$. The shoulder of this peak at lower binding energy of 529.9 eV was assigned to a contribution from oxygen bonded to titanium on the MXene without the presence of nearby fluorine atoms. At higher binding the component at 531.9 eV represents oxygen bonded to titanium where fluorine atoms occupy some of the other free positions around the Ti atom. It was shown that this position is also typical for –OH groups on the MXene surface [1]. The peak at 533.7 eV was assigned to adsorbed or intercalated water molecules. The peaks at 529.9 eV and 531.9 eV originating from MXene were modelled with asymmetrical line-shapes. The oxyfluoride and the water peaks were modelled by symmetrical gaussian-lorentzian line-shapes. One of the complications of fitting the O 1s spectra is the presence of oxygen bound to carbon in surface contamination. These tend to overlap in the O 1s spectrum with other contributions leading to overestimation of some components.

The core-level F 1s spectra are shown in **Figure S5**. A single asymmetrical component was fitted to represent the fluorine bound to titanium on the surface of the MXene as C—Ti—F. In the F 1s region many different species contribute to the signal at similar binding energies. The signal from fluorine in the oxyfluoride species $TiO_{2-x}F_{2x}$ is expected to overlap with the C—Ti—F species. It is therefore very difficult to distinguish between them. One indication could be slightly more symmetrical peak in the F 1s spectrum, as the $TiO_{2-x}F_{2x}$ are not conductive like MXene. This can be seen in the sample treated for 8 s in **Figure S5c**, where the asymmetrical line-shape that was used does not fit the measured data perfectly and the symmetrical component might be more suitable in this case.

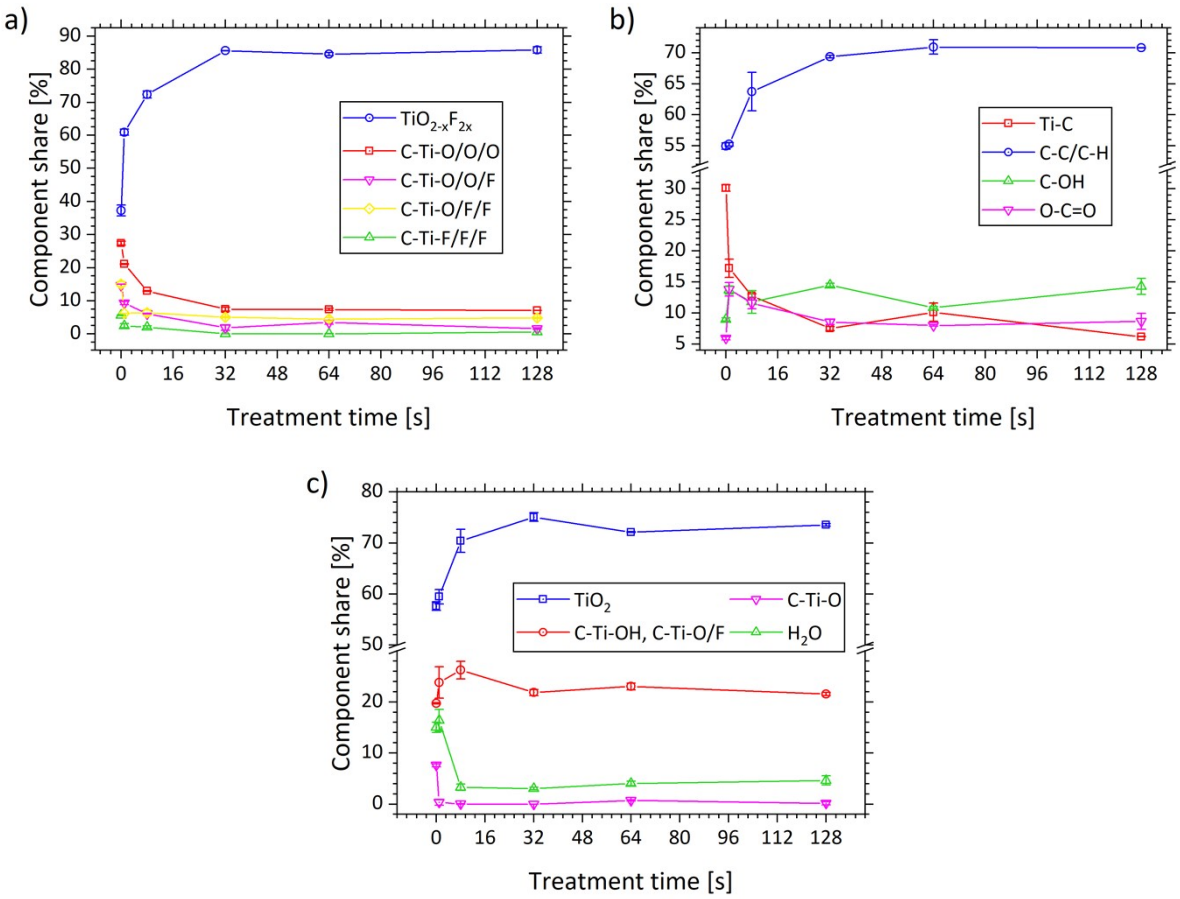

Figure S1. Evolution of components' shares obtained by fitting of **a)** Ti 2p, **b)** C 1s and **c)** O 1s core-level spectra of MXene films with plasma treatment of different duration.

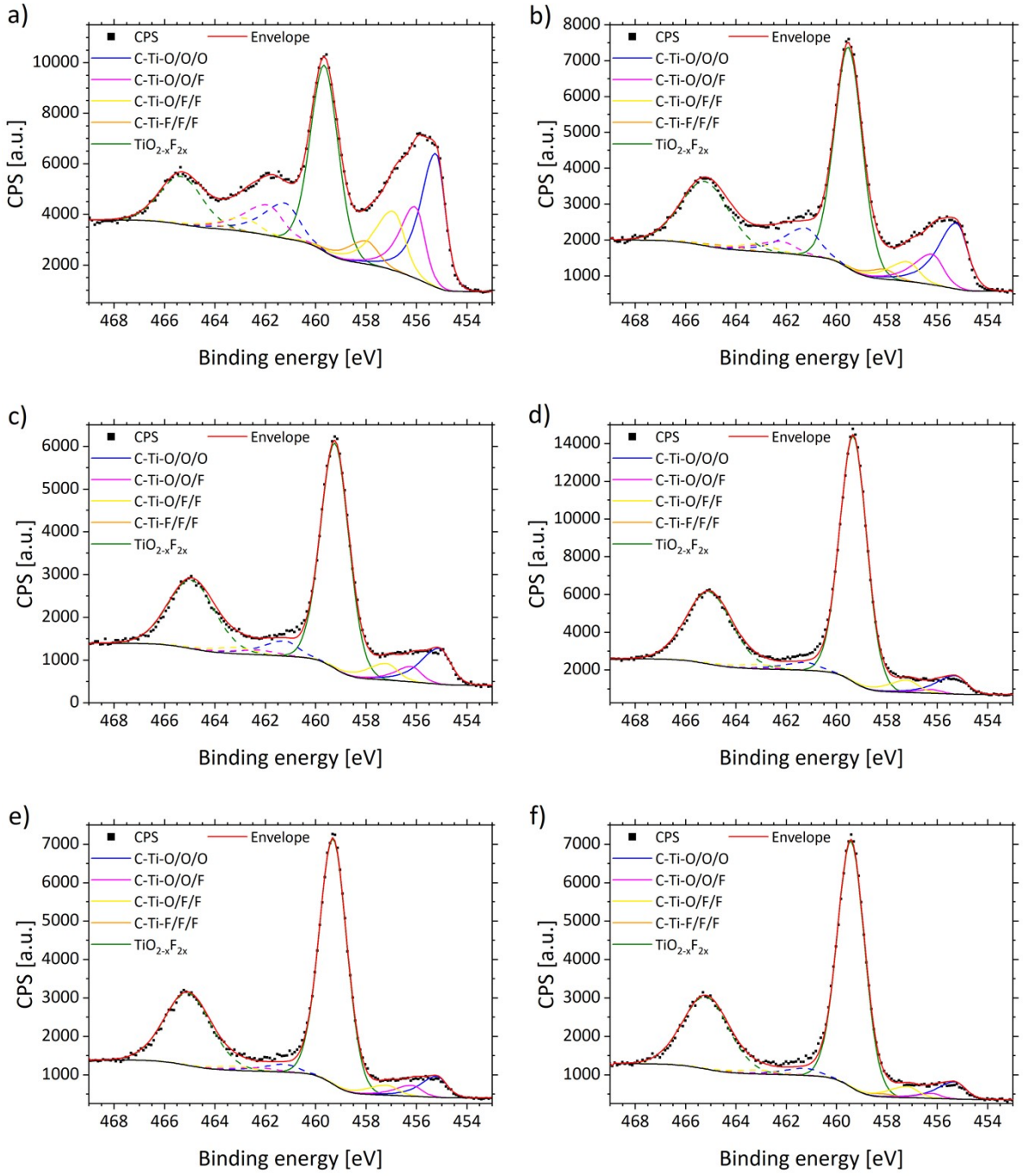

Figure S2. Deconvolutions of Ti 2p core-level spectra for **a)** reference, **b)** 1 s, **c)** 8 s, **d)** 32 s, **e)** 64 s and **f)** 128 s plasma-treated MXene film. The Ti 2p 3/2 components are drawn with solid line, the Ti 2p 1/3 are drawn with dashed line. Shirley background type was used. Asymmetrical line shape was used for C—Ti—O/O/O, C—Ti—O/O/F, C—Ti—O/F/F and C—Ti—F/F/F components and a symmetrical gaussian-lorentzian lineshape was used for the $TiO_{2-x}F_{2x}$ component.

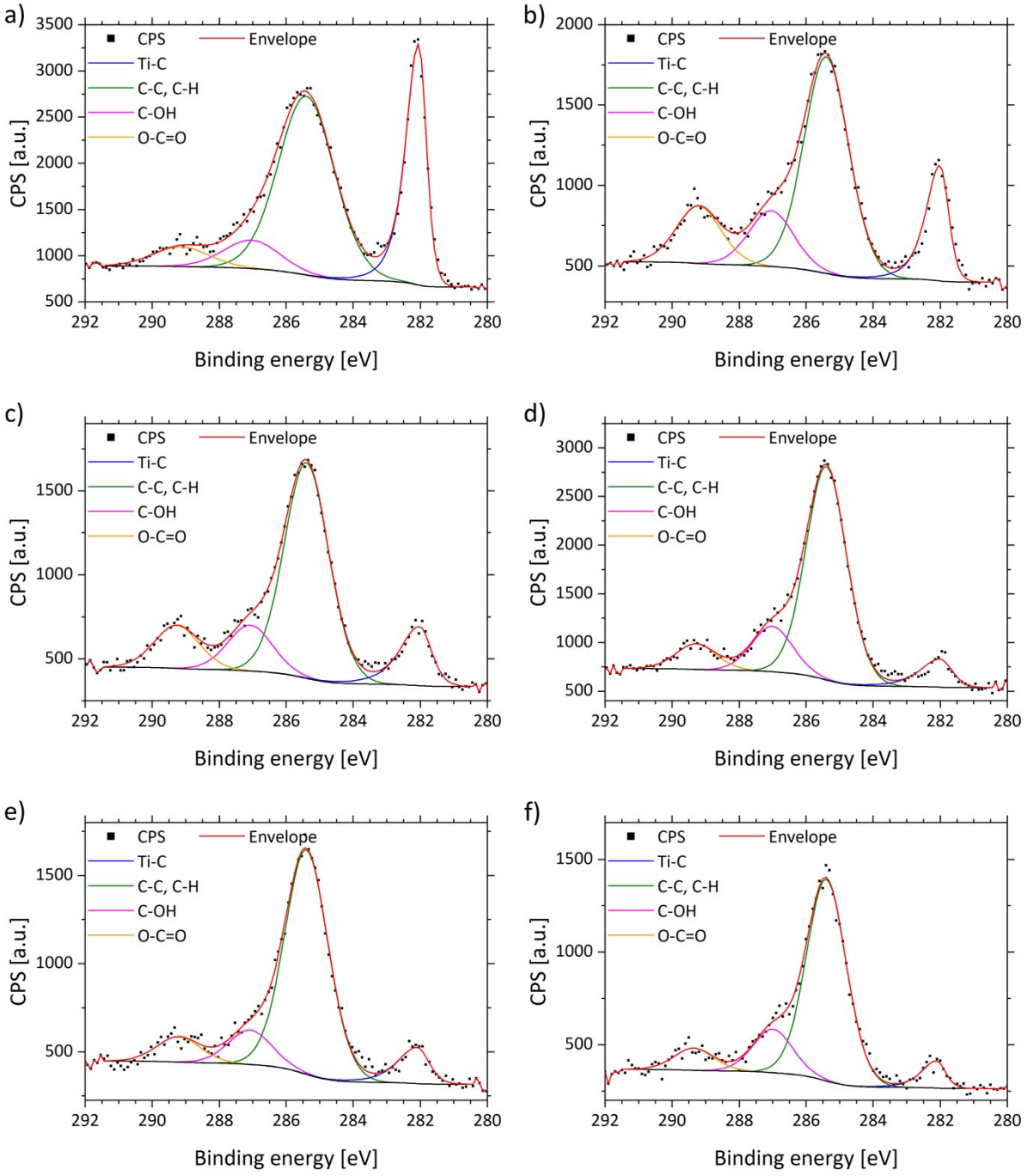

Figure S3. Deconvolutions of C1s core-level spectra for **a)** reference, **b)** 1 s, **c)** 8 s, **d)** 32 s, **e)** 64 s and **f)** 128 s plasma-treated MXene film. Shirley type background was used. Asymmetrical line shape was used for the Ti—C component and symmetrical gaussian-lorentzian line shape was used for the rest of the components.

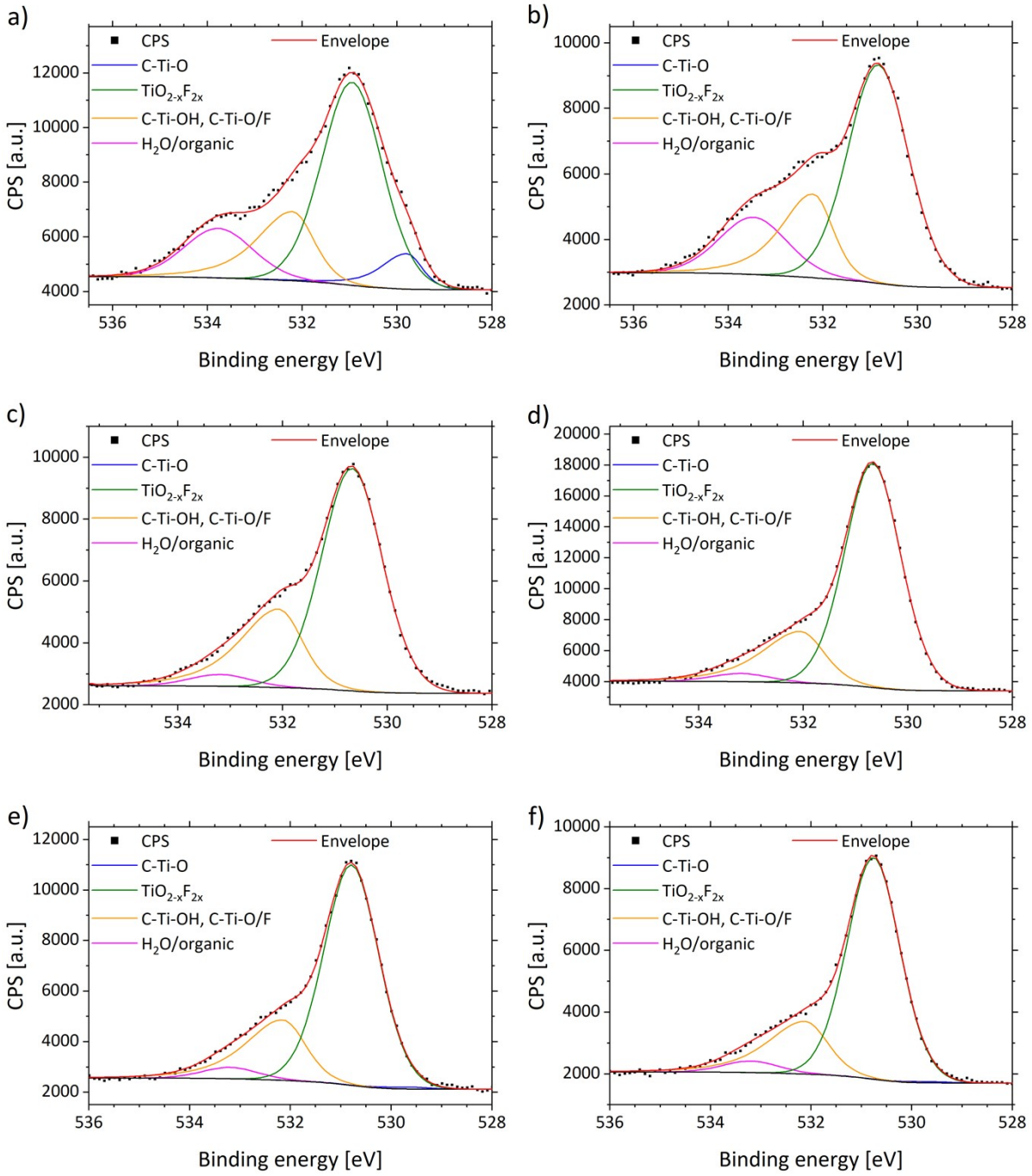

Figure S4. Deconvolutions of O1s core-level spectra for **a)** reference, **b)** 1 s plasma-treated, **c)** 8 s plasma-treated, **d)** 32 s plasma-treated, **e)** 64 s plasma-treated and **f)** 128 s plasma-treated MXene film. Shirley type background was used. Asymmetrical line shapes were used for C—Ti—O and C—Ti—OH components, symmetrical gaussian-lorentzian line shapes were used for $TiO_{2-x}F_{2x}$ and H_2O components.

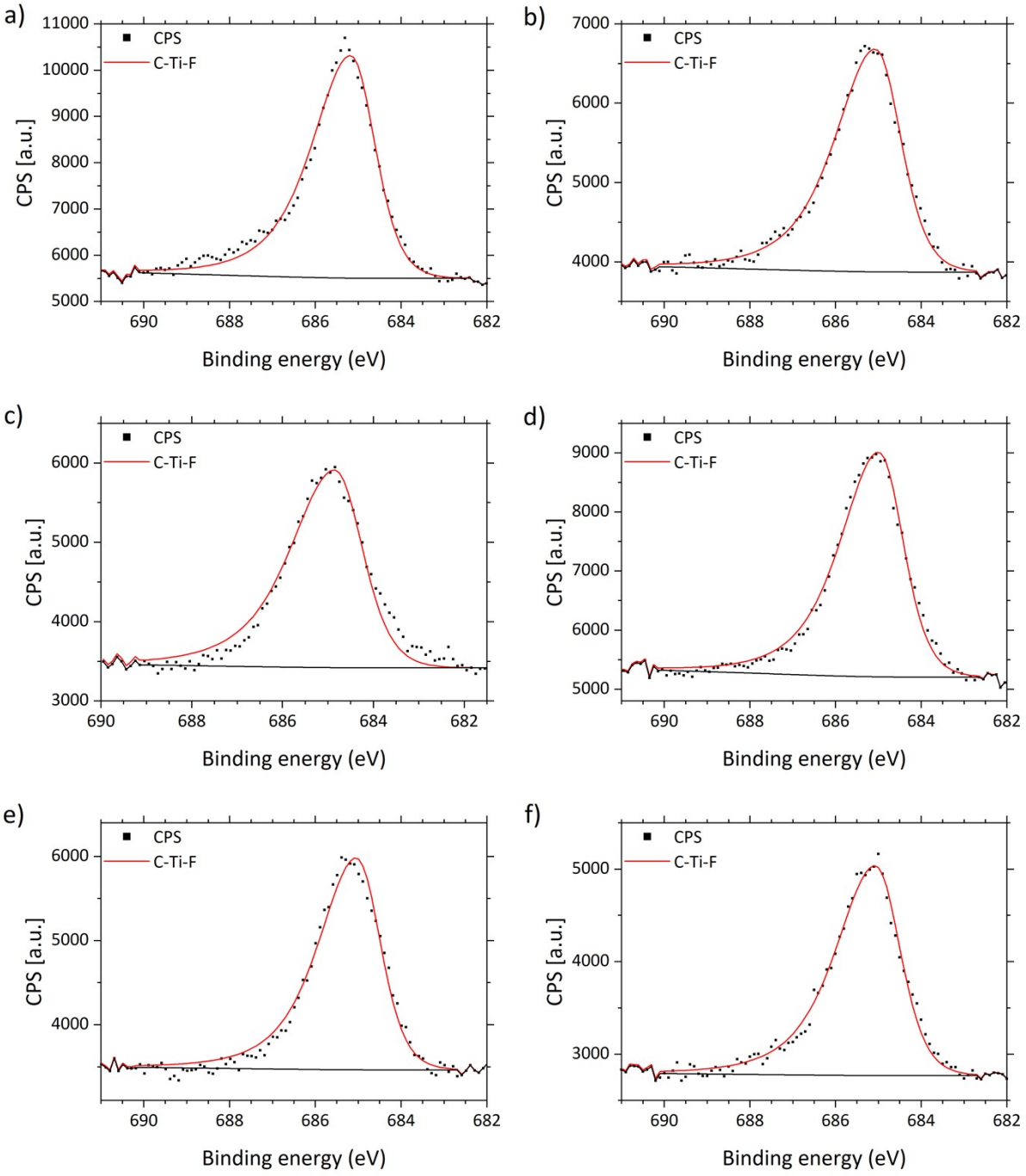

Figure S5. Deconvolutions of F1s core-level spectra for **a)** reference, **b)** 1 s plasma-treated, **c)** 8 s plasma-treated, **d)** 32 s plasma-treated, **e)** 64 s plasma-treated and **f)** 128 s plasma-treated MXene film. Shirley type background and asymmetrical line shape were used.

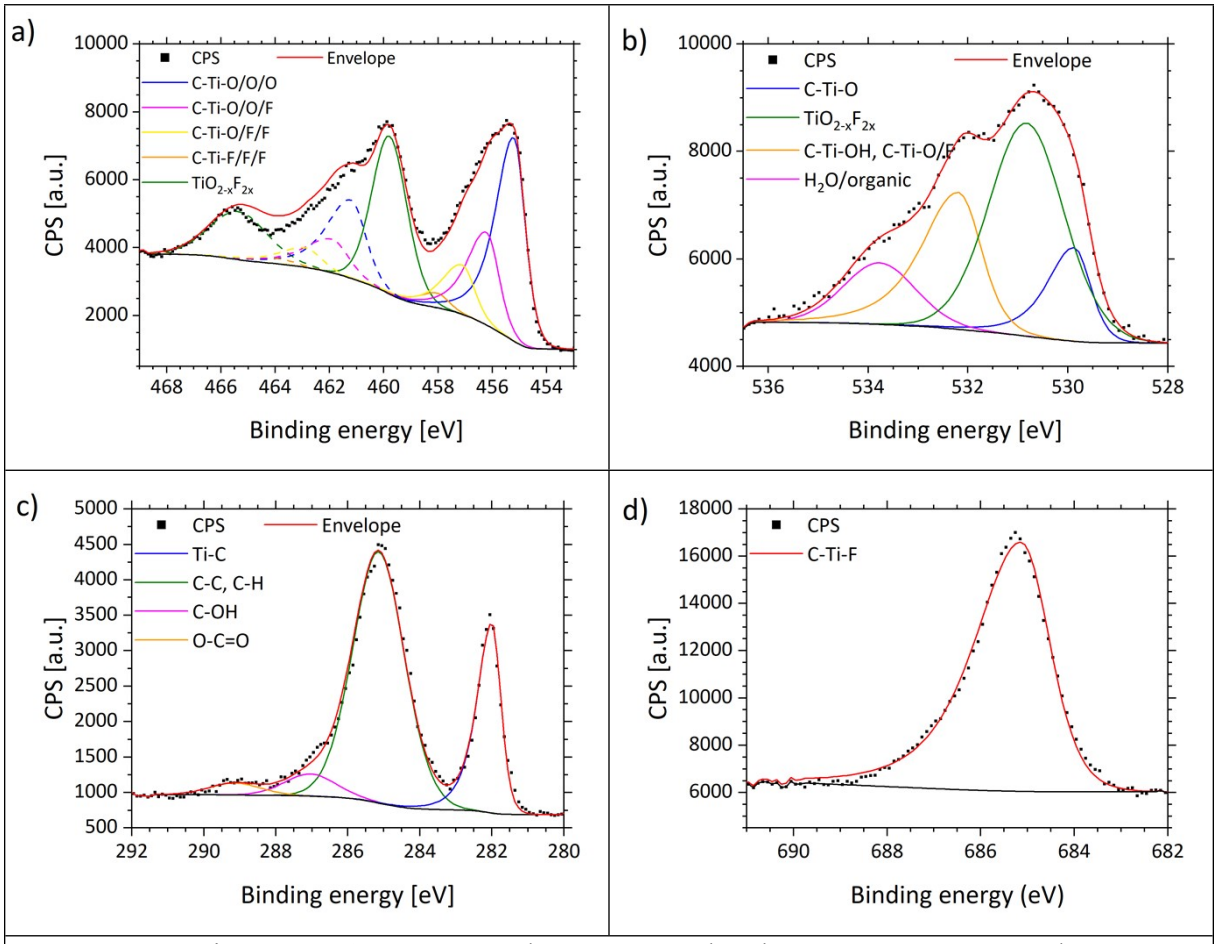

Figure S6. a) Ti 2p, **b)** O 1s, **c)** C 1s and **d)** F 1s core-level XPS spectra measured on MXene powder prior to the solution processing.

Morphology and structural analysis

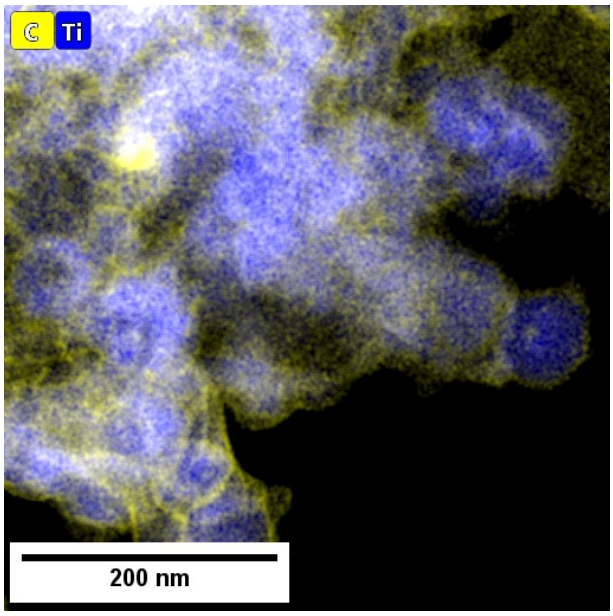

Figure S7. EDX from TEM image of the 128 s plasma treated MXene coating.

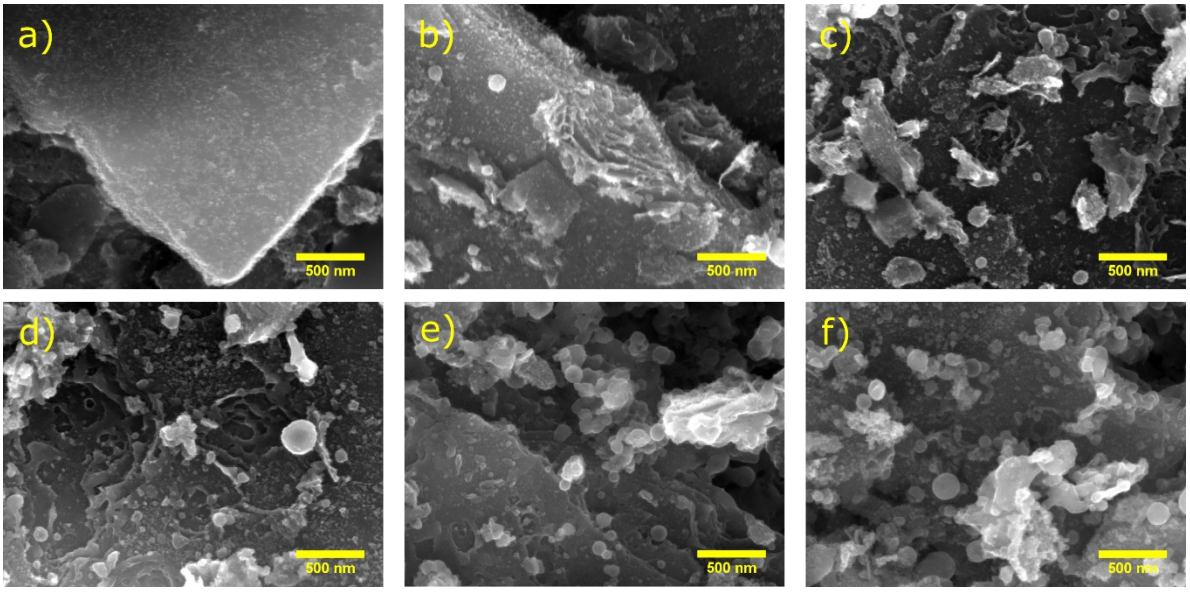

Figure S8. SEM images of MXene samples treated by oxygen plasma for various durations ranging from **a)** 0 s (reference) to **f)** 128 s.

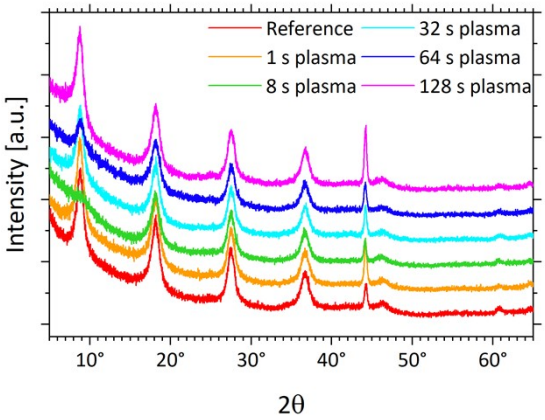

Figure S9. XRD diffractograms of MXene samples treated by oxygen plasma for various durations ranging from 0 s (reference) to 128 s.

Sheet resistance

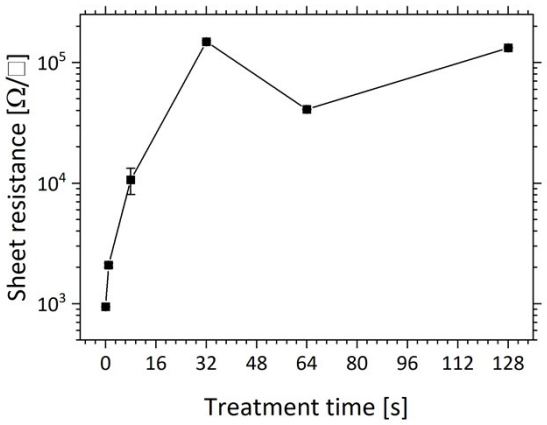

Figure S10. Sheet resistance of the untreated and plasma-treated MXene film as a function of treatment time.

Ab initio simulations

Methods

DFT calculations were performed by Vienna Ab initio Simulation Package – VASP [2–4] employing standard framework with Projector-Augmented-Wave (PAW) pseudopotentials and Perdew-Burke-Ernzerhof (PBE) exchange-correlation functional [5–7]. Plane wave energy cut-off was set to 650 eV and a Gamma-centred k-points grid with 0.1 $Å^{-1}$ spacing were used for all systems. A slab of Ti_3C_2 with single formula unit (5 atoms in unit cell) and a vacuum of 12 Å were used for the basic supercell. Terminating atoms or molecules were then set at approximate positions of the investigated binding sites and relaxed to 10^{-3} eV/Å.

Energies of adsorption for O, F and OH were calculated as energies of corresponding slab systems with respect to sums of energies of a clean Ti_3C_2 slab and isolated O_2, F_2 and O_2+H_2 molecules, respectively. Slab systems with terminations always contained two adsorbents per unit cell (one on each surface), corresponding to full coverage (surface saturation).

Core-level energies were calculated in the final-state approximation with half electron excited (Slater's transition state) [8,9]. Since VASP is inherently a valence electrons-only package, calculated core-level energies provide results that are suitable only for comparison of differences between the calculated core energies (core-level energy shifts), while absolute values are generally not accurate. We therefore fixed the positions of the calculated O-1s and F-1s core states to the most stable binding sites that were identified from calculations of adsorption energies – to the A site values of O-1s and F 1s core states in the C—Ti—O and C—Ti—F environments in Ti_3C_2.

Results

Surface of Ti_3C_2/Ti_2C nanosheets in fabricated MXene is typically terminated by oxygen, fluorine and OH, while the exact composition and presence of defects depends on the etching conditions during layers separation process [10–12]. There are several studies discussing the preferred adsorption sites for various atoms and molecules on MXene surfaces [12–17], which consider *fcc* hollow site (position A), *hcp* hollow sites (position B) and the TOP and BRIDGE positions.

Adsorption energies

All theoretical studies find that the most energetically favourable position for both O and F is A-site followed by position B. However, there are some discrepancies regarding TOP and BRIDGE positions, where in some works these were found to be locally stable (but less preferred than A and B) [14,15], while in others were found to be utterly unstable (converging towards A or B sites during the structural relaxation) [12,16]. In our simulations O and F atoms in positions A, B and TOP converged, but the BRIDGE position was indeed found to be unstable, as it always tended to fall into the A site, even after multiple attempts with changing slightly the initial structure and relaxation parameters. This result is in agreement with observations in studies [12,16,17]. Calculated adsorption energies are summarized in Table S3.

Results in Table S3 show that the most preferred binding site for all adsorbents is the A position and the second most stable position is B. The TOP-site is always the least preferred, while for adsorption of O the energy

Tab S3 Calculated adsorption energies for A, B and TOP positions for adsorption of O, F and OH. A-site is preferred for all adsorbents, followed by the B site and TOP. For oxygen, TOP position is highly disfavoured.

$E_{adsorp.}$ [eV / form unit]	$Ti_3C_2O_2$	$Ti_3C_2F_2$	$Ti_3C_2(OH)_2$
A site	-9.63	-11.03	-11.87
B site	-8.20	-10.28	-11.33
TOP site	-4.32	-9.32	-9.83

difference with respect to A and B is so large that this position is very unlikely to occur. For F and OH, the preference of A and B over TOP is milder. Calculated energies for O and F adsorption are in good agreement with the study of Schultz et al. [14].

Core-energy shifts

From the corresponding relaxed structures, we calculated core-level energy shifts of O 1s and F 1s states. As for comparison with our XPS fits we set positions of the calculated core energies of O 1s and F 1s in the most stable A sites to the positions concluded by Natu *et al.* [1] (529.8 eV for O-1s in C-Ti-O and 685.2 eV for F-1s in C-Ti-F). All other O 1s and F 1s core state values are then visualized based on their shifts from these two calibration points, like in previous studies by Pang *et al.* [18]. Results are shown in Fig. S10.

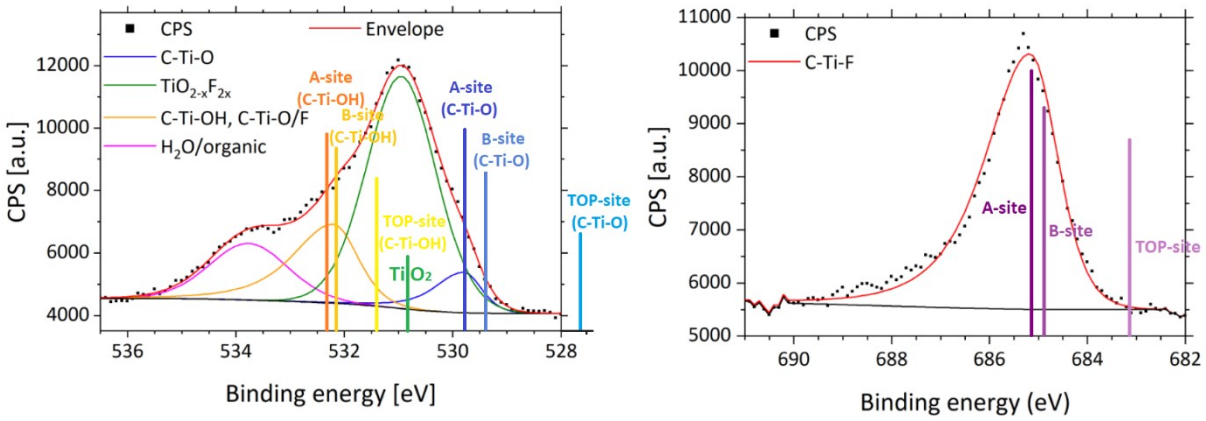

Figure S11. left) XPS spectra of O-1s states in the reference structure along the calculated O-1s core-level energy shifts for anatase-TiO_2 and A, B and TOP sites for adsorption of O and OH. Results of DFT simulations are calibrated to 529.8 eV for A-site. **right)** Spectra of F-1s states in reference MXene with DFT predictions set to 685.2 eV for the A-site, from which other F-1s states at different binding sites are shown. Relative heights of the bars showing DFT results correspond to relative adsorption energies between the adsorption sites calculated in Table S3.

Results in Fig. S10 show that adsorbents present on the surface of Ti_3C_2 always choose the most stable positions to bind, while the least stable ones seem to be not occupied at all. For example, oxygen TOP site is predicted to yield 2 eV lower O 1s core energy as A-site and there is indeed no sign of this position in the spectra. This corresponds well to fact that this site has only half the adsorption energy as the most stable A-site. At the same time, there is not a very strong preference for B sites over A, so it can be assumed that oxygen occupies A as well as some B sites. This is also in accordance with the predicted O 1s core states that differ only by ~0.3 eV.

Fitting only A or both A and B sites for our oxygen XPS spectra would therefore lead to similarly good fits. Both positions hence cannot be excluded and are probably present, at least to some extent.

Roughly the same conclusions can be drawn for the adsorption of OH, where the TOP position is predicted to have O 1s states 1 eV lower than for A-site, and this position is also apparently missing in the XPS spectra. Finally, adsorption of fluorine follows a similar pattern for F 1s states, where the energetically least favourable TOP position F-1s states lie about 2 eV lower than for position A, and are also clearly not present in our studied MXene sample.

Finally, we note that the above discussion is only a simplification of the real situation, since we are not considering the effect of having multiple O/F/OH terminations at the surface at once. Since they could be present in multiple possible combinations of the occupied A/B/TOP sites, this would complicate the calculations and discussion considerably, especially for the O-1s states, which are very close together and possibly could not be distinguished by the valence-electron theory.

References

[1] V. Natu, M. Benchakar, C. Canaff, A. Habrioux, S. Célérier, M. W. Barsoum, *Matter*. **2021**, *4* (4), 1224–1251. DOI: 10.1016/j.matt.2021.01.015.

[2] G. Kresse, J. Hafner, *Phys. Rev. B*. **1993**, *47* (1), 558. DOI: 10.1103/PhysRevB.47.558.

[3] G. Kresse, J. Furthmüller, *Comput. Mater. Sci.* **1996**, *6* (1), 15–50. DOI: 10.1016/0927-0256(96)00008-0.

[4] G. Kresse, J. Furthmüller, *Phys. Rev. B*. **1996**, *54* (16), 11169. DOI: 10.1103/PhysRevB.54.11169.

[5] P. E. Blöchl, *Phys. Rev. B*. **1994**, *50* (24), 17953. DOI: 10.1103/PhysRevB.50.17953.

[6] G. Kresse, D. Joubert, *Phys. Rev. B*. **1999**, *59* (3), 1758. DOI: 10.1103/PhysRevB.59.1758.

[7] J. P. Perdew, K. Burke, M. Ernzerhof, *Phys. Rev. Lett.* **1996**, *77* (18), 3865. DOI: 10.1103/PhysRevLett.77.3865.

[8] L. Köhler, G. Kresse, *Phys. Rev. B - Condens. Matter Mater. Phys.* **2004**, *70* (16), 1–9. DOI: 10.1103/PHYSREVB.70.165405/FIGURES/3/MEDIUM.

[9] N. Pueyo Bellafont, F. Viñes, W. Hieringer, F. Illas, *J. Comput. Chem.* **2017**, *38* (8), 518–522. DOI: 10.1002/JCC.24704.

[10] A. C. Y. Yuen, T. B. Y. Chen, B. Lin, W. Yang, I. I. Kabir, I. M. De Cachinho Cordeiro, A. E. Whitten, J. Mata, B. Yu, H. D. Lu, et al., *Compos. Part C Open Access*. **2021**, *5*, 100155. DOI: 10.1016/J.JCOMC.2021.100155.

[11] L. Chen, X. Ye, S. Chen, L. Ma, Z. Wang, Q. Wang, N. Hua, X. Xiao, S. Cai, X. Liu, *Ceram. Int.* **2020**, *46* (16), 25895–25904. DOI: 10.1016/J.CERAMINT.2020.07.074.

[12] J. Björk, J. Rosen, *Chem. Mater.* **2021**, *33* (23), 9108–9118. DOI: 10.1021/ACS.CHEMMATER.1C01264/ASSET/IMAGES/LARGE/CM1C01264_0008.JPEG.

[13] I. Persson, L.-Å. Näslund, J. Halim, M. W. Barsoum, V. Darakchieva, J. Palisaitis, J. Rosen, P. O. Å. Persson, *2D Mater.* **2017**, *5* (1), 015002. DOI: 10.1088/2053-1583/AA89CD.

[14] T. Schultz, N. C. Frey, K. Hantanasirisakul, S. Park, S. J. May, V. B. Shenoy, Y. Gogotsi, N. Koch, *Chem. Mater.* **2019**, *31* (17), 6590–6597. DOI: 10.1021/acs.chemmater.9b00414.

[15] L. Y. Gan, D. Huang, U. Schwingenschlögl, *J. Mater. Chem. A*. **2013**, *1* (43), 13672–13678. DOI: 10.1039/C3TA12032E.

[16] X.-T. Gao, Y. Xie, X.-D. Zhu, K.-N. Sun, X.-M. Xie, Y.-T. Liu, J.-Y. Yu, B. Ding, *Small*. **2018**, *14* (41), 1802443. DOI: 10.1002/SMLL.201802443.

[17] E. Yang, H. Ji, J. Kim, H. Kim, Y. Jung, *Phys. Chem. Chem. Phys.* **2015**, *17* (7), 5000–5005. DOI: 10.1039/C4CP05140H.

[18] Y. Pang, X. Zhou, E. I. Vovk, C. Guan, S. Li, A. P. van Bavel, Y. Yang, *Appl. Surf. Sci.* **2021**, *548*, 149214. DOI: 10.1016/J.APSUSC.2021.149214.